

## Current Developments of Mixed Conducting Membranes on Porous Substrates

Priscila Lemes-Rachadel<sup>a</sup>, Giuliani Sachinelli Garcia<sup>a</sup>, Ricardo Antonio Francisco Machado<sup>a</sup>,

Dachamir Hotza<sup>a\*</sup>, João Carlos Diniz da Costa<sup>b</sup>

<sup>a</sup>Department of Chemical Engineering – EQA, Federal University of Santa Catarina – UFSC,  
CEP 88040-900, Florianópolis, SC, Brazil

<sup>b</sup>Films and Inorganic Membrane Laboratory – FIMLab, School of Chemical Engineering,  
The University of Queensland – UQ, Brisbane, Australia

Received: March 11, 2013; Revised: September 7, 2013

The fabrication of mixed ionic-electronic conducting (MIEC) ceramic-based membranes for oxygen separation has extensively increased in the last three decades as a promising alternative of clean energy delivery. In recent years, the interest on supported MIEC membranes has increased due to their attractive properties such as higher mechanical strength and oxygen flux compared to self-supported membranes. This work presents a literature review on the development of supported MIEC membranes of perovskite structure. The concepts and transport mechanism of those membranes are explained and recent works on supported MIEC membranes are presented. Finally, manufacturing methods of self-supported membranes and their influence on oxygen permeation are discussed.

**Keywords:** *perovskite, MIEC, porous substrates, self-supported membranes*

### 1. Introduction

The reduction of CO<sub>2</sub> emissions due to electric power generation is one of the global challenges currently. Carbon capture and storage (CCS) is an approach to relieve global warming by capturing CO<sub>2</sub> and storing it instead of releasing it into the atmosphere<sup>1-4</sup>. Different fossil fuel power plant concepts for CCS are currently being developed, such as oxyfuel power plants. In this process, the fossil fuel is combusted using pure oxygen and the result is a gas stream with almost pure CO<sub>2</sub> (90-95%) in the dried flue gas. The CO<sub>2</sub> can then be captured more easily than when air is used in the combustion process and stored in a safe geological site<sup>5</sup>.

Mixed ionic-electronic conducting (MIEC) membranes are promising alternatives for oxyfuel power plants due to their high selectivity for oxygen separation and their significantly lowest efficiency losses compared with currently existing cryogenic distillation technology for oxygen separation<sup>6</sup>. The MIEC family is rich in structures and the perovskite structure is within them. The perovskite structure exhibits good ionic and electronic conductivity leading to attractive oxygen flux<sup>7</sup>. In the last decade, intensive research has been dedicated to the preparation and characterization of MIEC membranes<sup>1-18</sup>. However, a few reports can be found regarding to the preparation of crack-free membranes (with thicknesses less than 25 µm) for planar or tubular geometries.

Based on the Wagner equation<sup>7</sup>, the oxygen flux through a mixed-conducting dense membrane can be increased by reducing the thickness of the membrane until its thickness becomes less than a characteristic value at which the oxygen

flux is simultaneously determined by the bulk diffusion and surface exchange kinetics. The surface exchange kinetics involves different elementary steps such as: adsorption, dissociation and reduction of O<sub>2</sub><sup>[19]</sup>. Therefore, the improvement of O<sub>2</sub> permeation flux in the controlled surface system involves increasing the available surface area for the exchange process as well as the increase of catalytic properties of the membrane top layer. In this case, when the membrane thickness becomes very low, a porous support is needed for mechanical stability, particularly in the case of planar membranes. Thin porous catalytic layers can be also deposited on the other side of surface membrane to assist the increase of the available surface area for the exchange process.

Hence, in recent years the interest in the supported MIEC membranes has increased. The membranes that have been investigated vary widely in terms of thickness (10-500 µm) and chemical composition<sup>20</sup>. Catalytic layers are also employed in some cases. A major challenge in processing supported MIEC membranes is the selection of a suitable fabrication method and material for the porous substrate, taking into account requirements as chemical compatibility, similar thermal expansion coefficient (TEC), good mechanical strength and porosity for adequate diffusion of gas.

This review paper aims to assess the concepts of perovskite MIEC membranes and relate them to the manufacturing process of MIEC membranes on porous substrates. Recent works on supported MIEC membranes as well as main fabrication methods are reported and discussed.

\*e-mail: [dhotza@gmail.com](mailto:dhotza@gmail.com)

## 2. MIEC membranes

### 2.1. Concept

The two main types of oxygen separation systems based on ceramic membranes are mixed ionic–electronic conducting membranes (MIEC membranes) and pure oxygen conducting membranes (for example, solid electrolytes for solid oxide fuel cells (SOFC electrolytes)). An advantage of the MIEC membranes is that those membranes require no electrodes to operate as in SOFC electrolytes<sup>7,21</sup>. The MIEC membranes also stand out due to its potential application of high purity oxygen production.

The oxygen separation is performed at high temperatures, typically 800–900 °C and high O<sub>2</sub> flux are observed in dense membranes and with a perovskite structure<sup>22</sup>. As shown in Figure 1, the electronic conductivity is presented as a small internal circuit involving oxygen partial pressure gradient. The O<sub>2</sub> permeates from the high oxygen partial pressure side to the low oxygen partial pressure side, while the overall charge neutrality is maintained by opposite movement of electron flow<sup>23</sup>.

### 2.2. Structure

The general crystal structure of an ideal perovskite, ABO<sub>3</sub>, is cubic and is shown in Figure 2. The A-site ion may be a rare earth, alkali or alkaline earth ion, such as La, Na, Ca, Sr or Ba. The B-site ion is a transition metal, such as Fe, Co, Ni or Cu<sup>22</sup>.

The relative sizes of the A and B ions dictate the shape of the crystal structure. The perovskite structure is maintained if the value of tolerance factor (*t*) is between 0.75 e 1 (Equation 1) as proposed by Goldschmidt in 1927<sup>[24]</sup>:

$$t = \frac{R_A + R_O}{\sqrt{2}(R_B + R_O)} \quad (1)$$

where  $R_A$ ,  $R_B$  e  $R_O$  are the ratios of A-site, B-site and oxygen ions, respectively.

In crystals several types of defects can be present including zero dimensional or point defects. Those defects are generally separated into vacancies (particles missing in the lattice), interstitial particles (particles on lattice sites which are not normally occupied) and substitutional particles (lattice site that are occupied by foreign particles). The diffusion of oxygen ions is provided by vacancy defects present in the perovskite structure, because the ideal structure is unable of conducting those ions<sup>22,25</sup>. The presence of vacancies is due to the high tolerance of perovskite materials to non-stoichiometric structures, which allows obtaining a high ionic conduction of oxygen<sup>26</sup>.

When the A-site of the perovskite is doped with a metal ion with lower valence state, oxygen vacancies are created as well as a change in valence state of ions B occurs, in order to maintain electronic neutrality. The stability of perovskite structure oxides is also improved by doping B-site with a more stable ion to produce  $A_x A'_{1-x} B_y B'_{1-y} O_{3-\delta}$ . It is important to note that the term  $\delta$  is regarded as the number of vacancies or defects; therefore, the higher number of vacancies, higher will be oxygen permeation flux<sup>27</sup>. A large number of oxygen vacancies can be formed in perovskite crystals by doping of

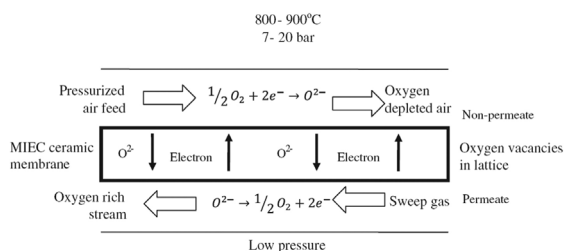


**Figure 1.** Schematic representation of O<sub>2</sub> transport in dense ceramic MIEC membranes<sup>7</sup>.

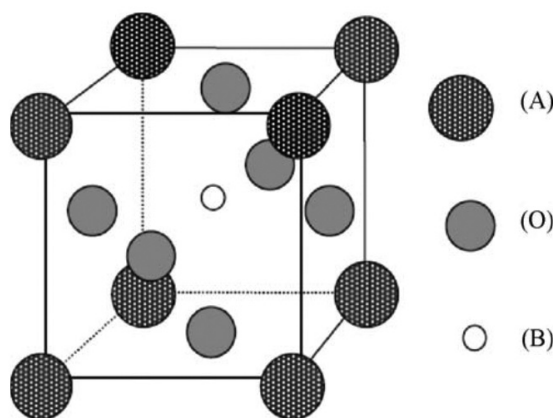


**Figure 2.** General structure of perovskite<sup>1</sup>.

ions with different valences. At high temperatures, oxygen is incorporated into perovskite crystal structure resulting in the annihilation of an oxygen vacancy and the formation of two electron holes, as expressed as in Equation 2.



where  $V_o^{\bullet\bullet}$  is the oxygen vacancy,  $O_O^x$  is the lattice oxygen and  $h^{\bullet}$  is the electron hole<sup>25</sup>.

### 2.3. Transport mechanism

According to the literature<sup>28-31</sup>, the oxygen transport through a MIEC membrane can occur by five stages, as follows (Figure 3):

- Mass transfer of gaseous O<sub>2</sub> from the gas stream to the membrane surface (high-pressure side.  $\uparrow p'_{O_2}$ );
- Adsorption of O<sub>2</sub> molecules followed by dissociation into ions (surface reaction of interface I);
- Transport of oxygen ions through the membrane (bulk diffusion in MIEC);
- Association of oxygen ions followed by desorption of oxygen molecules (surface reaction of interface II);
- Mass transfer of O<sub>2</sub> from the membrane surface to the gas stream (low-pressure side.  $\downarrow p'_{O_2}$ ).

The stages *b*, *c*, and *d* are the most important in this process. Stages *b* and *d* are governed by the kinetics surface exchange reactions (interfaces I and II) and stage *c* by the properties of bulk transport (bulk diffusion). For a MIEC membrane, the factor that limits the rate of O<sub>2</sub> permeation

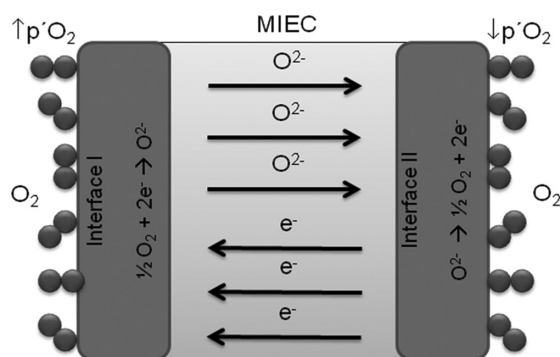


Figure 3. Oxygen transport through a MIEC membrane.

is the region at which the highest resistance occurs. The level of resistance in the interfaces I and II is affected by the nature of the material, such as the composition of perovskite or the exposed surface area. The resistance across the bulk diffusion is proportional to the thickness. For a relative thick membrane, the region of highest resistance is the region of the bulk diffusion. The oxygen permeation flux based on bulk diffusion can be expressed by Wagner equation<sup>7</sup>:

$$J_{O_2} = \frac{RT}{16F^2 L} \int_{p''_{O_2}}^{p'_{O_2}} \sigma_{amb}(pO_2) d \ln pO_2 \quad (3)$$

where  $J_{O_2}$  is the oxygen permeation flux in  $\text{mol m}^{-2} \text{s}^{-1}$ ;  $R$  is the gas constant;  $F$  is the Faraday constant;  $L$  is the membrane thickness;  $\sigma_{amb}$  is the ambipolar conductivity; and  $p'_{O_2}$  and  $p''_{O_2}$  are the oxygen partial pressures at the high pressure side and low pressure side, respectively.

Consequently, reducing membrane thickness will lead an increasing of  $O_2$  permeation rate. However, for thinner membranes, the resistance to oxygen ion conduction will be decreased until a certain limit, known as the characteristic thickness of the membrane ( $L_c$ ), which also depends on the operating conditions such as temperature and  $O_2$  partial pressure. The  $L_c$  of most MIEC membranes typically range from 20 to 3000  $\mu\text{m}$ <sup>32</sup>. For a thickness under  $L_c$ , the region of higher resistance becomes the interfaces I and II that are the surfaces with exchange reactions. The Wagner equation is not applicable when the oxygen flux becomes determined by the surface reaction.

Other mechanisms and relations have been proposed to explain the oxygen flux within this regime<sup>33,34</sup>. Surface exchange reactions are expected to be composed of sequential steps which might limit the overall rate. They may consist of adsorption from the gas phase, charge transfer reaction between the adsorbed species and bulk, including the reversed reactions<sup>19</sup>. For this point, a big challenge is finding a mathematical model to explain explicitly both the limiting cases such as bulk diffusion and surface exchange reactions, especially in the case of dense and thin planar MIEC membranes deposited on porous supports and/or modified surfaces.

### 3. Supported MIEC Membranes

To increase the mechanical strength of thinner ceramic membranes in operational conditions as elevated temperatures and high  $O_2$  partial pressure gradients, an alternative proposed by Bouwmeester et al.<sup>35</sup> is the membrane deposition via different techniques on porous substrates specially prepared. As previously mentioned, the porous substrate strongly influences the properties of the thin MIEC membrane layer, regardless of which deposition technique is used and must satisfy the following requisites:

- Chemical stability at fabrication temperature and in the fabrication atmosphere;
- Similar TEC to membrane layer materials;
- Chemical stability at membrane application temperature (800-900 °C) under operation atmosphere;
- Permeability that does not dominate the rate of permeation for gas diffusion;
- High mechanical strength at membrane application temperature.

Thin perovskites MIEC membrane have been deposited on porous supports using different techniques, e.g. dry pressing<sup>36-44</sup>, dip coating<sup>45-48</sup>, screen printing<sup>49,50</sup>, spray pyrolysis<sup>51</sup>, slip casting<sup>52</sup>, tape casting<sup>20,53-56</sup> and others<sup>57-63</sup>. Table 1 lists some of these studies including membrane and support fabrication method, material used for both components, as well as their thickness, pore-forming agent and pore size of the support and oxygen permeation fluxes in different operating conditions.

Chang et al.<sup>37</sup> produced crack-free dense MIEC membranes on porous supports via dry pressing by embedding 40% SCFZ ( $\text{SrCo}_{0.4}\text{Fe}_{0.5}\text{Zr}_{0.1}\text{O}_{3-\delta}$ ) onto MgO-based support and 40% MgO onto SCFZ membrane to avoid TEC problems between both materials. It was observed that the  $O_2$  flux is ten times higher in the supported MIEC membrane than in the self-supported membrane due to reducing of thickness. In another work<sup>36</sup> this group verified that  $O_2$  flux is also dependent on the direction of the permeation, i.e., the oxygen flux is higher when permeates in the support-membrane direction, due to increasing surface exchange rate on the dense layer in the high partial pressure side. In other groups an improvement of the oxygen permeation flux in supported MIEC membranes produced by dry pressing was also observed by modifying the microstructure of porous support to straight pores in order to favor gas diffusion<sup>41</sup>, by adding a thin porous activity layer in the permeate membrane side to increase surface area for accelerating surface exchange reaction in the low pressure side<sup>39</sup>. Kawahara et al.<sup>48</sup> employed dip coating to produce thin and dense perovskite membranes on porous substrates produced by dry pressing. It was noticed that higher  $O_2$  fluxes were achieved by reducing membrane thickness and controlling porosity in the porous substrate.

Baumann et al.<sup>20</sup> produced thin (70  $\mu\text{m}$ ) perovskite membranes on porous supports via tape casting and co-firing. In this case, the porous substrate offered a certain resistance to  $O_2$  flux and the deposition of a thin porous activity layer improved drastically the  $O_2$  permeation flux by varying operational conditions as temperature,  $O_2$  partial pressure and gas flow rates. Figure 4a-d shows SEM images of the cross-sections of those membranes after oxygen permeation

**Table 1.** MIEC membranes on porous substrates: materials and properties.

Membrane/ Support Material*	Membrane/ Support Process	Pore former	Pore size ( $\mu\text{m}$ )	Membrane/Support thickness ( $\mu\text{m}$ )	$J_{\text{O}_2}$ ( $\text{mol}\cdot\text{s}^{-1}\cdot\text{cm}^{-2}$ )	Ref.
SCFZ-0.4MgO/ MgO- 0.4SCFZ	Dry pressing	Active carbon	0.8	200/1000	$2.02\times 10^{-7}$ (900 °C)	[37]
BSCF	Dry pressing	Inorganic	1.18	200/1300	$6.17\times 10^{-7}$ (850 °C)	[39]
SCFZ	Dry pressing	Graphite, starch	5-30	500/1400	$1.78\times 10^{-7}$ (930 °C)	[43]
BSCF	Dry pressing	Graphite	3-20	170/1050	$1.2\times 10^{-6}$ (900 °C)	[44]
LSTF	Dry pressing	Organic	10	50-70/400	$8.41\times 10^{-6}$ (1000 °C)	[48]
LSCF	Screen printing/ Warm pressing	Organic	1.4	10-20/1200	$0.5\times 10^{-7}$ (900 °C)	[49]
LSCF	Slip casting/ Dry pressing	Methyl cellulose	0.5	200/1500	$1.41\times 10^{-7}$ (800 °C)	[51]
BSCF	Tape casting	Starch	2-25	70/830	$5.04\times 10^{-5}$ (900 °C)	[20]
LSFG/ LSF	Tape casting	Starch	8-20	80/1000	$1.19\times 10^{-8}$ (900 °C)	[55]
LSFG	Tape casting	Starch	8-20	120/820	$1.12\times 10^{-7}$ (920 °C)	[56]
CSTF	Spin coating/ Dry pressing	Carbon black	10-50	35/500	$1.56\times 10^{-6}$ (950 °C)	[57]
LCC	Slurry dropping/ Dry pressing	Oxalate	1-3	10/1200	$3.54\times 10^{-6}$ (930 °C)	[59]
LCC-BFZ/ LCC	Slurry dropping/ Dry pressing	Oxalate	1-3	30/1200	$1.19\times 10^{-6}$ (780 °C)	[60]
BLF	Slurry dropping/ Dry pressing	Oxalate	1-2	46/500-1000	$1.78\times 10^{-5}$ (930 °C)	[61]

\*BFZ =  $\text{BaFe}_{0.975}\text{Zr}_{0.025}\text{O}_{3-\delta}$ ; BLF =  $\text{Ba}_{0.95}\text{La}_{0.05}\text{FeO}_{3-\delta}$ ; BSCF =  $\text{Ba}_{0.5}\text{Sr}_{0.5}\text{Co}_{0.8}\text{Fe}_{0.2}\text{O}_{3-\delta}$ ; CSTF =  $\text{Ca}_{0.8}\text{Sr}_{0.2}\text{Ti}_{0.7}\text{Fe}_{0.3}\text{O}_{3-\delta}$ ; LCC =  $\text{La}_{0.6}\text{Ca}_{0.4}\text{CoO}_{3-\delta}$ ; LSCF =  $\text{La}_{0.58}\text{Sr}_{0.4}\text{Co}_{0.2}\text{Fe}_{0.8}\text{O}_{3-\delta}$ ; LSF =  $\text{La}_{0.8}\text{Sr}_{0.2}\text{FeO}_{3-\delta}$ ; LSFG =  $\text{La}_{0.6}\text{Sr}_{0.4}\text{Fe}_{0.9}\text{Ga}_{0.1}\text{O}_{3-\delta}$ ; LSTF =  $\text{La}_{0.6}\text{Sr}_{0.4}\text{Ti}_{0.3}\text{Fe}_{0.7}\text{O}_{3-\delta}$ ; SCFZ =  $\text{SrCo}_{0.4}\text{Fe}_{0.5}\text{Zr}_{0.1}\text{O}_{3-\delta}$ .

measurements. A suitable adhesion of the dense membrane on porous support may be observed, Figure 4a, b, as well as the thin (17  $\mu\text{m}$ ) porous active layer deposited by screen printing, Figure 4c, d. The highest  $\text{O}_2$  fluxes values achieved in the case of porous activity layer deposition are due to increased available surface area in the membrane, since the limiting factor becomes the surface exchange reaction when the membrane thickness is too thin, depending on the characteristic value ( $L_c$ ) of each material. Watanabe et al.<sup>59</sup> have used slurry dropping deposition technique to produce thinner (10-30  $\mu\text{m}$ ) perovskite membranes on porous support. Higher  $\text{O}_2$  fluxes were measured in supported MIEC membranes with porous active layer deposited on the low partial pressure side when compared with supported membranes without active layer and even lower values for self-supported membranes.

In almost all revised works, such as in those with highest oxygen permeation fluxes showed in Table 1, the authors used the same material for membrane and substrate. The same approach was applied to active layers to avoid differences of thermal expansion coefficient (TEC), thereby preventing delamination and cracks during sintering and operating conditions. Table 1 also shows that the average pore size in the support materials varies from < 1  $\mu\text{m}$  to around 50  $\mu\text{m}$ . Within this range it can be observed that the average pore size had no significant influence on the  $\text{O}_2$  flux results. High oxygen flux results were found either for smaller (1-2  $\mu\text{m}$ )<sup>61</sup> or larger pores (5-25  $\mu\text{m}$ )<sup>20</sup>.

An important aspect is to ensure an open and interconnected porosity, providing the adequate permeability for gas diffusion. The most of studies employed the

sacrificial template technique to create porosity in support material. This concept is based on incorporating an organic agent in the material composition to be removed in a slow thermal treatment after shaping and before sintering. In this context, it is interesting to select available routes for processing macroporous ceramics in order to find an inexpensive, environmentally friendly and suitable method for the manufacture of porous supports. An extensive review on processing techniques of macroporous ceramics and its relationship to control the porosity was made by Studart et al.<sup>64</sup> Further information can be found elsewhere<sup>65-70</sup>.

A more recent and innovative method to fabricate ultra thin MIEC membranes, different of those proposed for planar configurations, is the formation of asymmetric hollow fibers via an immersion induced phase inversion and sintering techniques. These hollow fibers might be processed with very thin and dense skin layer integrated on the porous support of the same perovskite material. In addition to its ability to support very thin walled membranes, the hollow fiber geometry also maximizes the surface area per unit volume. Recent developments show large improvements in oxygen permeation rates in hollow fibers<sup>1,12,13,15,17,18</sup> compared with flat, self-supported membranes. Similar results might be compared with some of the best results in the literature on flat supported membranes. Hollow fiber membranes can be fabricated using simple processing steps, without the use of porous substrate. Perovskite capillaries with an outer diameter from 0.5 to 3 mm and wall thicknesses from 50 to 500  $\mu\text{m}$  have been manufactured<sup>12,13</sup>. However, material



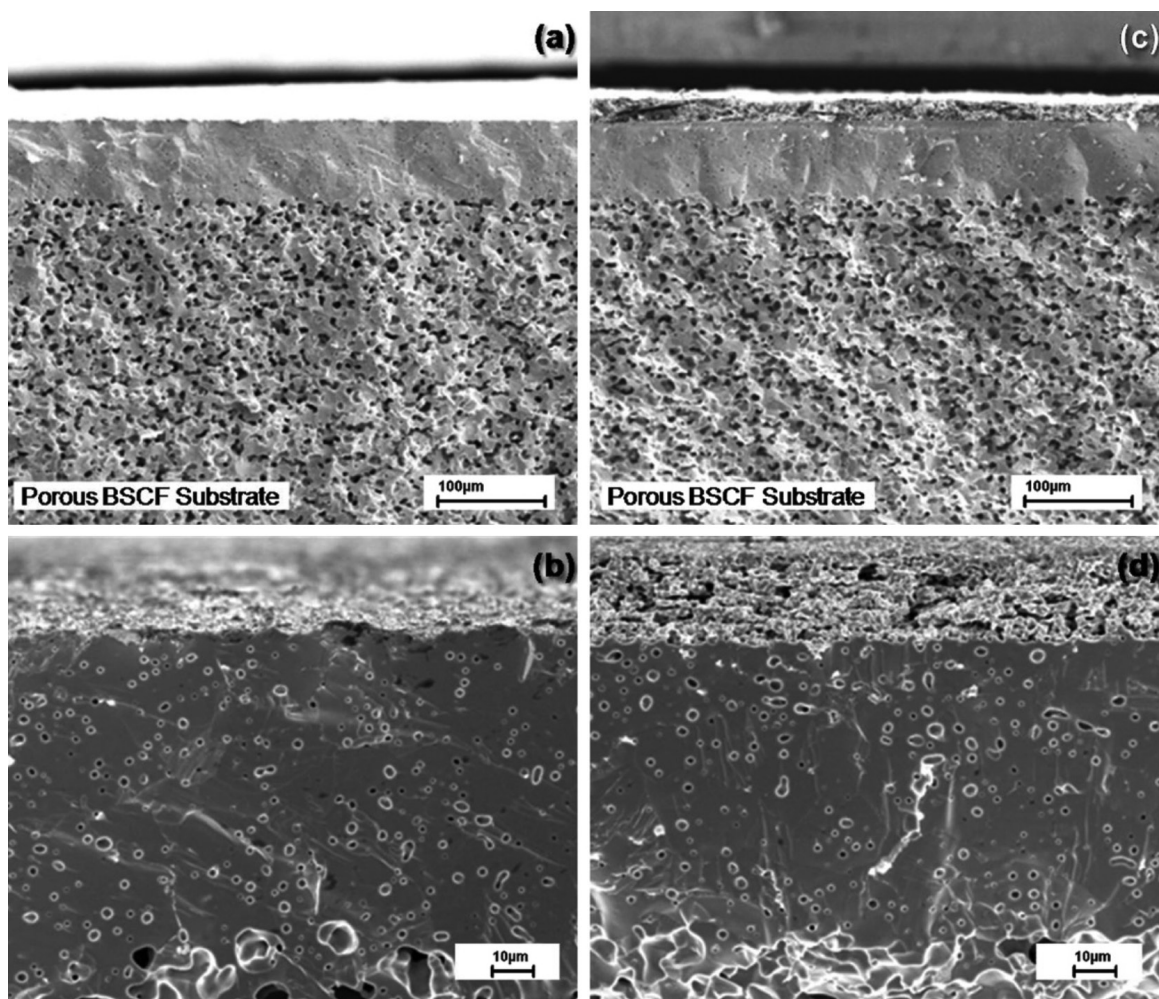


**Figure 4.** Fracture cross-sections (SEM images) of two membranes after oxygen permeation measurements: (a and b) without oxygen activity layer and (c and d) with an oxygen activation layer<sup>20</sup>.

strength limitation prevents wall thickness of hollow fiber membranes to be reduced further below 200  $\mu\text{m}$ .

#### 4. Conclusions

Dense perovskite membranes are promising alternatives to  $\text{O}_2$  separation and  $\text{CO}_2$  capture in oxy-combustion plants. Improvements in the design of these membranes are being intensively studied and flat configurations of supported MIEC membranes produced with the same material adding a thin porous activity layer has achieved good improvements regarding oxygen flux. The deposition of the membrane may be accomplished by simple methods as dip coating, tape casting and slurry dropping. Besides the need for

chemical compatibility and mechanical strength at operating conditions, the porous substrate must be engineered in order not to limit diffusion of gas by controlling its porosity and microstructure. The key point for further improvements in the planar supported MIEC membranes is the definition of an explicit model for explaining the surface exchange reactions of these supported membranes and controlling the porosity and microstructure of the porous substrate.

#### Acknowledgements

Capes, CNPq and Petrobras are gratefully acknowledged for financial support.

## References

1. Leo A, Liu S and Diniz da Costa JC. Development of mixed conducting membranes for clean coal energy delivery. *International Journal of Greenhouse Gas Control*. 2009; 3(4):357-367. <http://dx.doi.org/10.1016/j.ijggc.2008.11.003>
2. Chen Z, Ran R, Shao Z, Yu H, Diniz da Costa JC and Liu S. Further performance improvement of  $\text{Ba}_{0.5}\text{Sr}_{0.5}\text{Co}_{0.8}\text{Fe}_{0.2}\text{O}_{3-\delta}$  perovskite membranes for air separation. *Ceramics International*. 2009; 35(6):2455-2461. <http://dx.doi.org/10.1016/j.ceramint.2009.02.015>
3. Baumann S, Schulze-Kuppers F, Roitsch S, Betz M, Zwick M, Pfaff EM et al. Influence of sintering conditions on microstructure and oxygen permeation of  $\text{Ba}_{0.5}\text{Sr}_{0.5}\text{Co}_{0.8}\text{Fe}_{0.2}\text{O}_{3-\delta}$  (BSCF) oxygen transport membranes. *Journal of Membrane Science*. 2010; 359(1-2):102-109. <http://dx.doi.org/10.1016/j.memsci.2010.02.002>
4. Haworth P, Smart S, Glasscock J and Diniz da Costa JC. Yttrium doped BSCF membranes for oxygen separation. *Separation and Purification Technology*. 2011; 81(1):88-93. <http://dx.doi.org/10.1016/j.seppur.2011.07.007>
5. Stadler HB, Habermehl F, Persigehl M, Kneer B, Modigell R and Jeschke M. Oxyfuel coal combustion by efficient integration of oxygen transport membranes. *International Journal of Greenhouse Gas Control*. 2011; 5: 7-14. <http://dx.doi.org/10.1016/j.ijggc.2010.03.004>
6. Cziperek MZ, Bouwmeester HJM, Modigell M, Ebert K, Voigt I, Meulenberg WA et al. Gas separation membranes for zero emission fossil power plants: MEM-BRAIN. *Journal of Membrane Science*. 2010; 359:149-159. <http://dx.doi.org/10.1016/j.memsci.2010.04.012>
7. Sunarso J, Baumann S, Serra JM, Meulenberg WA, Lius S, Lin YS et al. Mixed ionic-electronic conducting (MIEC) ceramic-based membranes for oxygen separation. *Journal of Membrane Science*. 2008; 320(1-2):13-41. <http://dx.doi.org/10.1016/j.memsci.2008.03.074>
8. Bouwmeester HJM, Kruidhof H, Burggraaf AJ and Gellings PJ. Oxygen semipermeability of erbium-stabilized bismuth oxide. *Solid State Ionics*. 1992; 53-56:460-468. [http://dx.doi.org/10.1016/0167-2738\(92\)90416-M](http://dx.doi.org/10.1016/0167-2738(92)90416-M)
9. Skinner SJ and Kilner JA. Oxygen diffusion and surface exchange in  $\text{La}_{2-x}\text{Sr}_x\text{NiO}_{4+\delta}$ . *Solid State Ionics*. 2000; 135:709-712. [http://dx.doi.org/10.1016/S0167-2738\(00\)00388-X](http://dx.doi.org/10.1016/S0167-2738(00)00388-X)
10. Ji Y, Kilner JA and Carolan MF. Electrical properties and oxygen diffusion in yttria-stabilised zirconia (YSZ)- $\text{La}_{0.8}\text{Sr}_{0.2}\text{MnO}_{3+\delta}$  (LSM) composites. *Solid State Ionics*. 2005; 176:937-943. <http://dx.doi.org/10.1016/j.ssi.2004.11.019>
11. Kharton VV, Kovalevsky AV, Viskup AP, Shaula AL, Figueiredo FM, Naumovich EM et al. Oxygen transport in  $\text{Ce}_{0.8}\text{Gd}_{0.2}\text{O}_{2-\delta}$  based composite membranes. *Solid State Ionics*. 2003; 160:247-258. [http://dx.doi.org/10.1016/S0167-2738\(03\)00183-8](http://dx.doi.org/10.1016/S0167-2738(03)00183-8)
12. Schiestel T, Kilgus M, Peter S, Caspary KJ, Wang H and Caro J. Hollow fibre perovskite membranes for oxygen separation. *Journal of Membrane Science*. 2005; 258:1-4. <http://dx.doi.org/10.1016/j.memsci.2005.03.035>
13. Wang H, Werth S, Schiestel T and Caro J. Perovskite hollow-fibre membranes for the production of oxygen-enriched air. *Angewandte Chemie International Edition*. 2005; 44(42):6906-6909. PMID:16206306. <http://dx.doi.org/10.1002/anie.200501914>
14. Buysse C, Kovalevsky A, Snijders F, Buekenhoudt A, Mullens S, Luyten J et al. Fabrication and oxygen permeability of gastight, macrovoid-free  $\text{Ba}_{0.5}\text{Sr}_{0.5}\text{Co}_{0.8}\text{Fe}_{0.2}\text{O}_{3-\delta}$  capillaries for high temperature gas separation. *Journal of Membrane Science*. 2010; 359:86-92. <http://dx.doi.org/10.1016/j.memsci.2009.10.030>
15. Leo A, Smart S, Liu S and Diniz da Costa JC. High performance perovskite hollow fibres for oxygen separation. *Journal of Membrane Science*. 2011; 368(1-2):64-68. <http://dx.doi.org/10.1016/j.memsci.2010.11.002>
16. Serra JM, Vert VB, Büchler O, Meulenberg WA and Buchkremer HP. IT-SOFC supported on mixed oxygen ionic-electronic conducting composites. *Chemistry of Materials*. 2008; 20(12): 3867-3875. <http://dx.doi.org/10.1021/cm702508f>
17. Liu S and Gavallas GR. Oxygen selective ceramic hollow fiber membranes. *Journal of Membrane Science*. 2005; 246:103-108. <http://dx.doi.org/10.1016/j.memsci.2004.09.028>
18. Li K, Tan X and Liu Y. Single-step fabrication of ceramic hollow fibers for oxygen permeation. *Journal of Membrane Science*. 2006; 272: 1-5. <http://dx.doi.org/10.1016/j.memsci.2005.11.053>
19. Chen CS, Boukamp BA, Bouwmeester HJM, Cao GZ, Kruidhof H, Winnubst AJA et al. Microstructural development, electrical-properties and oxygen permeation of zirconia-palladium composites. *Solid State Ionics*. 1995; 76(1-2):23-28. [http://dx.doi.org/10.1016/0167-2738\(94\)00253-O](http://dx.doi.org/10.1016/0167-2738(94)00253-O)
20. Baumann S, Serra JM, Lobera MP, Escolástico S, Schulze-Küppers F and Meulenberg WA. Ultrahigh oxygen permeation flux through supported  $\text{Ba}_{0.5}\text{Sr}_{0.5}\text{Co}_{0.8}\text{Fe}_{0.2}\text{O}_{3-\delta}$  membranes. *Journal of Membrane Science*. 2011; 377(1-2):198-205. <http://dx.doi.org/10.1016/j.memsci.2011.04.050>
21. Smart S, Lin CXC, Ding L, Thambimuthu K and Diniz da Costa JC. Ceramic membranes for gas processing in coal gasification. *Energy and Environmental Science*. 2010; 3:268-278. <http://dx.doi.org/10.1039/b924327e>
22. Burggraaf AJ and Cot L. *Fundamentals of Inorganic Membrane Science and Technology*. New York: Elsevier; 1996.
23. Badwal SPS and Ciacchi FT. Ceramic membrane technologies for oxygen separation. *Advanced Materials*. 2001; 13(12-13):993-996. [http://dx.doi.org/10.1002/1521-4095\(200107\)13:12/13<993::AID-ADMA993>3.0.CO;2#](http://dx.doi.org/10.1002/1521-4095(200107)13:12/13<993::AID-ADMA993>3.0.CO;2#)
24. Goldschmidt VM. *Geochemische Verteilungsgesetze der Elemente*. Oslo: Norske Videnska; 1927. PMID:17771601.
25. Adler SB, Chen XY and Wilson JR. Mechanisms and rate laws for oxygen exchange on mixed-conducting oxide surfaces. *Journal of Catalysis*. 2007; 245(1):91-109. <http://dx.doi.org/10.1016/j.jcat.2006.09.019>
26. Bhatia S, Hashim SM and Mohamed AR. Current status of ceramic-based membranes for oxygen separation from air. *Advances in Colloid and Interface Science*. 2010; 160(1-2):88-100. PMID:20813344. <http://dx.doi.org/10.1016/j.cis.2010.07.007>
27. Yang WS, Wang HH and Cong Y. Oxygen permeation study in a tubular  $\text{Ba}_{0.5}\text{Sr}_{0.5}\text{Co}_{0.8}\text{Fe}_{0.2}\text{O}_{3-\delta}$  oxygen permeable membrane. *Journal of Membrane Science*. 2002; 210(2): 259-271. [http://dx.doi.org/10.1016/S0376-7388\(02\)00361-7](http://dx.doi.org/10.1016/S0376-7388(02)00361-7)
28. Ishihara T, Kilner JA, Honda M, Sakai N, Yokokawa H and Takita Y. Oxygen surface exchange and diffusion in  $\text{LaGaO}_3$  based perovskite type oxides. *Solid State Ionics*. 1998; 113:593-600. [http://dx.doi.org/10.1016/S0167-2738\(98\)00390-7](http://dx.doi.org/10.1016/S0167-2738(98)00390-7)
29. Manning PS, Sirman JD and Kilner JA. Oxygen self-diffusion and surface exchange studies of oxide electrolytes having the fluorite structure. *Solid State Ionics*. 1996; 93(1-2):125-132. [http://dx.doi.org/10.1016/S0167-2738\(96\)00514-0](http://dx.doi.org/10.1016/S0167-2738(96)00514-0)

30. Ruiz-Trejo E, Siman JD, Baikov YM and Kilner JA. Oxygen ion diffusivity, surface exchange and ionic conductivity in single crystal Gadolinia doped Ceria. *Solid State Ionics*. 1998; 113:565-569. [http://dx.doi.org/10.1016/S0167-2738\(98\)00323-3](http://dx.doi.org/10.1016/S0167-2738(98)00323-3)
31. Lane JA and Kilner JA. Oxygen surface exchange on gadolinia doped ceria. *Solid State Ionics*. 2000; 136:927-932. [http://dx.doi.org/10.1016/S0167-2738\(00\)00530-0](http://dx.doi.org/10.1016/S0167-2738(00)00530-0)
32. Aasland S, Tangen IL, Wiik K and Odegard R. Oxygen permeation of  $\text{SrFe}_{0.67}\text{Co}_{0.33}\text{O}_{3-\delta}$ . *Solid State Ionics*. 2000; 135(1-4):713-717. [http://dx.doi.org/10.1016/S0167-2738\(00\)00389-1](http://dx.doi.org/10.1016/S0167-2738(00)00389-1)
33. Lin YS, Wang WJ and Han JH. Oxygen permeation through thin mixed-conducting solid oxide membranes. *AIChE Journal*. 1994; 40(5):786-798. <http://dx.doi.org/10.1002/aic.690400506>
34. Tan XY, Liu SM and Hughes R. Theoretical analysis of ion permeation through mixed conducting membranes and its application to dehydrogenation reactions. *Solid State Ionics*. 2000; 138(1-2):149-159. [http://dx.doi.org/10.1016/S0167-2738\(00\)00782-7](http://dx.doi.org/10.1016/S0167-2738(00)00782-7)
35. Bouwmeester HJ, Kruidhof MH and Burggraaf AJ. Importance of the surface exchange kinetics as rate-limiting step in oxygen permeation through mixed-conducting oxides. *Solid State Ionics*. 1994; 72:185-194. [http://dx.doi.org/10.1016/0167-2738\(94\)90145-7](http://dx.doi.org/10.1016/0167-2738(94)90145-7)
36. Chang XF, Zhang C, Dong X, Yang C, Wanqin J and Xu N. Experimental and modeling study of oxygen permeation modes for asymmetric mixed-conducting membranes. *Journal of Membrane Science*. 2008; 322(2):429-435. <http://dx.doi.org/10.1016/j.memsci.2008.05.061>
37. Chang XF, Zhang C, Jin W and Xu N. Match of thermal performances between the membrane and the support for supported dense mixed-conducting membranes. *Journal of Membrane Science*. 2006; 285(1-2):232-238. <http://dx.doi.org/10.1016/j.memsci.2006.08.025>
38. Chen ZH, Shao ZP, Ran R, Zhou W, Zeng PY and Liu SM. A dense oxygen separation membrane with a layered morphologic structure. *Journal of Membrane Science*. 2007; 300(1-2):182-190. <http://dx.doi.org/10.1016/j.memsci.2007.05.023>
39. Kovalevsky AV, Yaremchenko AA, Kolotygin VA, Shaula AL, Kharton VV, Snijkers FMM et al. Processing and oxygen permeation studies of asymmetric multilayer  $\text{Ba}_{0.5}\text{Sr}_{0.5}\text{Co}_{0.8}\text{Fe}_{0.2}\text{O}_{3-\delta}$  membranes. *Journal of Membrane Science*. 2011; 380(1-2):68-80. <http://dx.doi.org/10.1016/j.memsci.2011.06.034>
40. Kovalevsky AV, Yaremchenko AA, Kolotygin VA, Snijkers FMM, Kharton VV, Buekenhoudt A et al. Oxygen permeability and stability of asymmetric multilayer  $\text{Ba}_{0.5}\text{Sr}_{0.5}\text{Co}_{0.8}\text{Fe}_{0.2}\text{O}_{3-\delta}$  ceramic membranes. *Solid State Ionics*. 2011; 192(1):677-681. <http://dx.doi.org/10.1016/j.ssi.2010.05.030>
41. Ikeguchi M, Ishii K, Sekine Y, Kikuchi E and Matsukata M. Improving oxygen permeability in  $\text{SrFeCo}_{0.5}\text{O}_x$  asymmetric membranes by modifying support-layer porous structure. *Materials Letters*. 2005; 59(11):1356-1360. <http://dx.doi.org/10.1016/j.matlet.2004.12.042>
42. Jiang QY, Nordheden KJ and Stagg-Williams SM. Oxygen permeation study and improvement of  $\text{Ba}_{0.5}\text{Sr}_{0.5}\text{Co}_{0.8}\text{Fe}_{0.2}\text{O}_x$  perovskite ceramic membranes. *Journal of Membrane Science*. 2011; 369(1-2):174-181. <http://dx.doi.org/10.1016/j.memsci.2010.11.073>
43. Chang XF, Zhang C, He Y, Dong X, Jin W and Xu N. A comparative study of the performance of symmetric and asymmetric mixed-conducting membranes. *Chinese Journal of Chemical Engineering*. 2009; 17(4):562-570. [http://dx.doi.org/10.1016/S1004-9541\(08\)60245-1](http://dx.doi.org/10.1016/S1004-9541(08)60245-1)
44. Kovalevsky AV, Kharton VV, Snijkers FMM, Coymans JFC, Luyten JJ and Frade JR. Processing and oxygen permeability of asymmetric ferrite-based ceramic membranes. *Solid State Ionics*. 2008; 179(1-6):61-65.
45. Hong L, Chen XF and Cao ZD. Preparation of a perovskite  $\text{La}_{0.2}\text{Sr}_{0.8}\text{CoO}_{3-x}$  membrane on a porous MgO substrate. *Journal of the European Ceramic Society*. 2001; 21(12):2207-2215. [http://dx.doi.org/10.1016/S0955-2219\(00\)00320-4](http://dx.doi.org/10.1016/S0955-2219(00)00320-4)
46. Lee S, Yu JH, Seo DW and Woo SK. Thick-film type oxygen transport membrane: Preparation, oxygen permeation and characterization. *Journal of Electroceramics*. 2006; 17(2-4):719-722. <http://dx.doi.org/10.1007/s10832-006-0388-x>
47. Ito W, Nagai T and Sakon T. Oxygen separation from compressed air using a mixed conducting perovskite-type oxide membrane. *Solid State Ionics*. 2007; 178(11-12):809-816. <http://dx.doi.org/10.1016/j.ssi.2007.02.031>
48. Kawahara A, Takahashi Y, Hirano Y, Hirano M and Ishihara T. Importance of pore structure control in porous substrate for high oxygen penetration in  $\text{La}_{0.6}\text{Sr}_{0.4}\text{Ti}_{0.3}\text{Fe}_{0.7}\text{O}_3$  thin film for  $\text{CH}_4$  partial oxidation. *Solid State Ionics*. 2011; 190(1):53-59. <http://dx.doi.org/10.1016/j.ssi.2010.12.015>
49. Xing Y, Bauman S, Sebold D, Ruttinger M, Venskutonis A, Meulenberg WA et al. Chemical compatibility investigation of thin-film oxygen transport membranes on metallic substrates. *Journal of the American Ceramic Society*. 2011; 94(3):861-866. <http://dx.doi.org/10.1111/j.1551-2916.2010.04171.x>
50. Buchler O, Serra JM, Meulenberg WA, Sebold D and Buchkremer HP. Preparation and properties of thin  $\text{La}_{1-x}\text{Sr}_x\text{Co}_{1-y}\text{Fe}_y\text{O}_{3-\delta}$  perovskitic membranes supported on tailored ceramic substrates. *Solid State Ionics*. 2007; 178(1-2):91-99. <http://dx.doi.org/10.1016/j.ssi.2006.11.015>
51. Abrutis A. Preparation of dense, ultra-thin MIEC ceramic membranes by atmospheric spray-pyrolysis technique. *Journal of Membrane Science*. 2004; 240(1-2):113-122. <http://dx.doi.org/10.1016/j.memsci.2004.03.043>
52. Jin WQ, Li S, Huang P, Xu N and Shi J. Preparation of an asymmetric perovskite-type membrane and its oxygen permeability. *Journal of Membrane Science*. 2001; 185(2):237-243. [http://dx.doi.org/10.1016/S0376-7388\(00\)00650-5](http://dx.doi.org/10.1016/S0376-7388(00)00650-5)
53. Middleton H, Diethelm S, Ihringer R, Larrain D, Sfeir J and Herle JV. Co-casting and co-sintering of porous MgO support plates with thin dense perovskite layers of  $\text{LaSrFeCoO}_3$ . *Journal of the European Ceramic Society*. 2004; 24(6):1083-1086. [http://dx.doi.org/10.1016/S0955-2219\(03\)00554-5](http://dx.doi.org/10.1016/S0955-2219(03)00554-5)
54. Fontaine ML, Smith JB, Larring Y and Bredesen R. On the preparation of asymmetric  $\text{CaTi}_{0.9}\text{Fe}_{0.1}\text{O}_{3-\delta}$  membranes by tape-casting and co-sintering process. *Journal of Membrane Science*. 2009; 326(2):310-315. <http://dx.doi.org/10.1016/j.memsci.2008.10.009>
55. Julian A, Juste E, Geffroy PM, Coudert V, Degot S, Del Gallo P et al. Elaboration of  $\text{La}_{0.8}\text{Sr}_{0.2}\text{Fe}_{0.7}\text{Ga}_{0.3}\text{O}_{3-\delta}/\text{La}_{0.8}\text{M}_{0.2}\text{FeO}_{3-\delta}$  (M = Ca, Sr and Ba) asymmetric membranes by tape-casting and co-firing. *Journal of Membrane Science*. 2009; 333(1-2):132-140. <http://dx.doi.org/10.1016/j.memsci.2009.02.002>
56. Etchegoyen G, Chartier T and Del-Gallo P. An architectural approach to the oxygen permeability of a  $\text{La}_{0.6}\text{Sr}_{0.4}\text{Fe}_{0.9}\text{Ga}_{0.1}\text{O}_{3-\delta}$  perovskite membrane. *Journal of the European Ceramic Society*. 2006; 26(13):2807-2815. <http://dx.doi.org/10.1016/j.jeurceramsoc.2005.06.025>
57. Araki S, Hoshi Y, Hamakawa S and Mizukami F. Synthesis and characterization of mixed ionic-electronic conducting



- $\text{Ca}_{0.8}\text{Sr}_{0.2}\text{Ti}_{0.7}\text{Fe}_{0.3}\text{O}_{3-\alpha}$  thin film. *Solid State Ionics*. 2008; 178(33-34):1740-1745. <http://dx.doi.org/10.1016/j.ssi.2007.11.011>
58. Araki S, Yamamoto H and Hoshi Y. Synthesis of  $\text{Ca}_{0.8}\text{Sr}_{0.2}\text{Ti}_{0.7}\text{Fe}_{0.3}\text{O}_{3-\delta}$  thin film membranes and its application to the partial oxidation of methane. *Solid State Ionics*. 2012; 221:43-49. <http://dx.doi.org/10.1016/j.ssi.2012.06.001>
  59. Watanabe K, Yuasa M, Kida T, Shimanoe K, Teraoka Y and Yamazoe N. Preparation of oxygen evolution layer/ $\text{La}_{0.6}\text{Ca}_{0.4}\text{CoO}_3$  dense membrane/porous support asymmetric structure for high-performance oxygen permeation. *Solid State Ionics*. 2008; 179(27-32): 1377-1381.
  60. Watanabe K, Yuasa M, Kida T, Shimanoe K, Teraoka Y and Yamazoe N. Oxygen Permeation of a dense/porous asymmetric membrane using  $\text{La}_{0.6}\text{Ca}_{0.4}\text{CoO}_{3-\delta}$ - $\text{BaFe}_{0.975}\text{Zr}_{0.025}\text{O}_{3-\delta}$  system. *Chemistry Letters*. 2009; 38(1):94-95. <http://dx.doi.org/10.1246/cl.2009.94>
  61. Watanabe K, Yuasa M, Kida T, Teraoka Y, Yamazoe N and Shimanoe K. High-Performance oxygen-permeable membranes with an asymmetric structure using  $\text{Ba}_{0.95}\text{La}_{0.05}\text{FeO}_{3-\delta}$  perovskite-type oxide. *Advanced Materials*. 2010; 22(21):2367-2370. PMID:20354973. <http://dx.doi.org/10.1002/adma.200903953>
  62. Matsuka M, Agranovski IE and Braddock RD. Preparation of asymmetric perovskite-type membranes by a settlement method. *Ceramics International*. 2010; 36(2):643-651. <http://dx.doi.org/10.1016/j.ceramint.2009.10.007>
  63. Sadykov V, Zarubina V, Pavlova S, Krieger T, Alilina G, Lukashovich A et al. Design of asymmetric multilayer membranes based on mixed ionic-electronic conducting composites supported on Ni-Al foam substrate. *Catalysis Today*. 2010; 156(3-4):173-180. <http://dx.doi.org/10.1016/j.cattod.2010.07.030>
  64. Studart AR, Gonzenbach UT, Tervoort E and Gauckler LJ. Processing routes to macroporous ceramics: A review. *Journal of the American Ceramic Society*. 2006; 89(6):1771-1789. <http://dx.doi.org/10.1111/j.1551-2916.2006.01044.x>
  65. Sepulveda P and Binner JG. Processing of cellular ceramics by foaming and in situ polymerisation of organic monomers. *Journal of the European Ceramic Society*. 1999; 19(12):2059-2066. [http://dx.doi.org/10.1016/S0955-2219\(99\)00024-2](http://dx.doi.org/10.1016/S0955-2219(99)00024-2)
  66. Innocentini MDM, Salvini VR, Macedo A and Pandolfelli VC. Prediction of ceramic foams permeability using Ergun's equation. *Materials Research*. 1999; 2(4):283-289. <http://dx.doi.org/10.1590/S1516-14391999000400008>
  67. Ortega FS, Innocentini MDM, Valenzuela FAO and Pandolfelli VC. Effect of aeration technique on the macrostructure and permeability of gelcast ceramic foams. *Cerâmica*. 2002; 48(306):79-85. <http://dx.doi.org/10.1590/S0366-69132002000200006>
  68. Prabhakaran K, Melkeri A, Gokhale NM and Sharma SC. Preparation of macroporous alumina ceramics using wheat particles as gelling and pore forming agent. *Ceramics International*. 2007; 33(1):77-81. <http://dx.doi.org/10.1016/j.ceramint.2005.07.020>
  69. Silveira CB, Escobar JA, Quintero MW, Sousa E, Moraes EG, Oliveira APN et al. Thermal decomposition of polyurethane foams for manufacturing LZSA cellular glass ceramics. *Química Nova*. 2007; 30(5):1104-1107. <http://dx.doi.org/10.1590/S0100-40422007000500010>
  70. Barg S, Soltmann C, Andrade M, Koch D and Grathwohl G. Cellular ceramics by direct foaming of emulsified ceramic powder suspensions. *Journal of the American Ceramic Society*. 2008; 91(9):2823-2829. <http://dx.doi.org/10.1111/j.1551-2916.2008.02553.x>